

# Transport and magnetic properties of Fe substituted manganites

M. L. CRAUS<sup>a,b</sup>, M. LOZOVAN<sup>a,\*</sup>, N. CORNEI<sup>c</sup>, C. MITA<sup>c</sup>

<sup>a</sup>National Institute of Research & Development for Technical Physics, Iassy, Romania

<sup>b</sup>Joint Institute for Nuclear Research, Dubna, Russia

<sup>c</sup>"Al. I. Cuza" University, Iassy, Romania

Magnetic perovskites with  $ABO_3$  structure have interesting properties, due their complex electronic phase diagram, which depend on chemical composition, average radius of A places and chemical disorder degree. We have obtained a new type of manganites, with  $La_{0.54}Ho_{0.11}(Ca, Sr)_{0.35}Mn_{1-x}Fe_xO_3$  chemical composition, were obtained by sol-gel method. XRD analysis was performed with at room temperature with a diffractometer previewed with a data acquisition system, data being handled with a Rietveld type program. The samples contain only an orthorhombic phase, identified as Pnma, GS 62. Lattice constants, unit cell volume and the atomic positions in the unit cell were determined. Mn-O distances and Mn-O-Mn angles were calculated and a correlation with the observed Curie temperatures was put in evidence. The magnetic measurements were performed between 77 and 300 K with a Foner type magnetometer. Electric measurements were performed by means of four probes method, between 7 and 300 K. Large values of magnetoresistance were obtained for samples with Sr.

(Received September 25, 2007; accepted February 7, 2008)

*Keywords:* Manganites, Transport properties, Magnetic properties, Magnetoresistance

## 1. Introduction

The discovery of anomalously large magnetoresistance around  $T_C$  and increasing of resistivity by substituting the Mn cations with other transitions cations has increase the interest to possible technical applications [1–3].

The electrical and magnetic properties of doped manganites can be controlled by varying average radius of A places/tolerance factor and by substitution of Mg with other transition cation [4]. Remarkably, paramagnetic insulator, ferromagnetic–metallic, and charge ordered–insulator temperature-dependent phase transitions are induced in the doped manganites.  $Nd_{0.67}Sr_{0.33}MnO_3$  is ferromagnet (FM) under 270 K, while  $Nd_{0.67}Sr_{0.33}FeO_3$  is an antiferromagnet (AFM) insulator, due to the Fe-O-Fe superexchange bonds. It could be interesting to observe the change of the magnetic and electric properties into a compound which changes from a ferromagnet to an antiferromagnet, due to the change of Mn/Fe concentrations. On other hand, the change of the alkaline earth cations on A places can significantly modify the MR due to the influence on the double-exchange (DE) interaction of distortion in the  $Mn^{3+}-O^{2-}-Mn^{4+}$  network, eventually by the magnetic coupling between the dopant and Mn ions [5, 6]. Local distortions of the  $MnO_6$  octahedra determine the charge transport behavior and complex magnetic and crystalline structures. The substitution of Mn with other transition cation destroys the DE interaction, by lowering the Curie temperature and enhancing the magnetoresistance; some authors obtained a large magnetoresistance by substituted Mn with M=Cr, Fe, Ni or Cu in  $La_{0.7}Sr_{0.3}Mn_{0.9}M_{0.1}O_3$  [5]. However the studies on the substituted with Fe manganites leads to idea that Fe encourages an antiferromagnetic insulator behavior,

opposed to the DE interactions [7]. Mössbauer studies on Fe doped  $La_{1-x}Ca_xMnO_3$  compounds indicated an antiferromagnetic coupling between Fe and its Mn neighbors [8]. The strains induced by the substitution of Mn with other transition cations or by substitution of Sr with Ca or Ba contribute to the magnetoresistance effect [9].

The substitution of Mn with Fe should not influence the crystalline structure, because the crystalline radii of these two cations are the same. However, a large difference exists between the  $Mn^{3+}$  and  $Fe^{3+}$  behavior: only  $Mn^{3+}$  is a Jahn-Teller (JT) cation and could induce a local strain in crystalline lattice. The presence of large amount of  $Mn^{3+}$  cations leads to a structural transition from a cubic to a lower symmetry. Implicitly, the presence of a large amount of non-JT cations decreases the concentration of crystalline distortions.

Previously we got and investigated La-Ca manganites and Nd-Sr manganites [10,11].

In this paper, we focused on the obtaining of  $La_{0.54}Ho_{0.11}(Ca, Sr)_{0.35}Mn_{1-x}Fe_xO_3$  manganites and the determination of the influence of the Fe and Ca cations on their magnetic and electric properties.

## 2. Experimental

The manganies with the chemical composition  $La_{0.54}Ho_{0.11}(Ca, Sr)_{0.35}Mn_{1-x}Fe_xO_3$  ( $x = 0.03; 0.06; 0.1; 0.15; 0.2$ ) were prepared by means of sol-gel method. The stoichiometric amounts of analytical reagents of  $La_2O_3$ ,  $Ho_2O_3$ ,  $Sr(CH_3COO)_2 \cdot 0.5H_2O$ ,  $Fe_2O_3$  and  $Mn(CH_3COO)_2 \cdot 4H_2O$  were dissolved in dilute  $HNO_3$  (1N) solution. The gel was obtained by adding a solution of citric acid. The solution was evaporated by heating, and brown solid gel was obtained. The gel was preheated in air

at 400°C for 5 h to remove the remaining organic materials, annealed at 800 °C for 17 h and then sintered at 1200°C for 12 h. The presintered and sintered samples were monitored by X-ray analysis, to determine begin of the solid-state reaction and the phase composition.

The magnetic and electric measurements were performed with a Foner type magnetometer, between 77 and 300K, respectively with a four probe method, between 7-300 K. UV-VIS-near IR measurements were performed with VSU-2P Karl Zeiss Jena spectrophotometer, between 200 – 1200 nm. The IR spectra were made including the sintered compounds in KBr disk; the transmittance has been measured with FT-IR JASCO 660 Plus spectrophotometer in the frequency range from 900 to 300  $\text{cm}^{-1}$

### 3. Results and discussions

The  $\text{La}_{0.54}\text{Ho}_{0.11}(\text{Sr}/\text{Ca})_{0.35}\text{Mn}_{1-x}\text{Fe}_x\text{O}_3$  (LHSMFO/LHCMFO) manganites were investigated by X-ray diffraction; the samples contain only one phase, orthorhombic with Pnma structure.

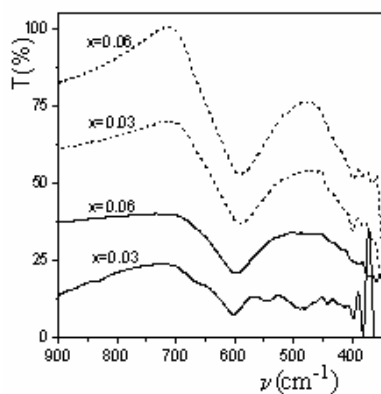


Fig. 1. Infrared transmission spectra for LHSMFO (solid lines) and LHCMFO (dashed lines) samples.

The vibrational spectra of perovskites have been described as the internal vibration of the octahedron containing highly charged and small Mn ion because of relatively weak Ln-O bonds. In 800-400  $\text{cm}^{-1}$  frequency range there are two infrared active vibrations modes for the  $\text{MnO}_6$  octahedra which are sensitive to the Mn-O bond length. The absorption peaks around 350  $\text{cm}^{-1}$  correspond to the bending mode of O-Mn-O bond angle.

The experimental FT-IR spectra (Fig. 1) show the expected main peaks in both region with an apparent splitting of the stretching mode band only for the LHSMFO ( $x=0.03$ ). This could be interpreted as a structural triplet allowed by the non-centrosymmetric  $\text{MnO}_6$  octahedric groups and the different covalent degree of the B (Mn,Fe)-O bonds. The maximum absorption bands shift to lower frequency (from 601  $\text{cm}^{-1}$  (main peak of LHSMFO,  $x=0.03$ ) to 589  $\text{cm}^{-1}$  (LHCMFO,  $x=0.06$ )). This increase may be, partially, ascribed to the size effect of Fe ions on B places ( $\text{Fe}^{3+}$  high spin  $r = 0.785 \text{ \AA}$ ) and the increase of symmetry of crystalline lattice of manganites.

The intensity of peaks increase with the increase of Fe content and the change of  $\text{Sr}^{2+}$  with  $\text{Ca}^{2+}$  cations. The symmetry of  $\text{MnO}_6$  groups is correlated with the existence of manganese ions into a mixture of two valence states,  $\text{Mn}^{3+}$  and  $\text{Mn}^{4+}$  and the Jahn-Teller effects (partly related to the average ionic radius and electronegativity of ions on the A sites). The presence of  $\text{Fe}^{3+}$  ions on the B places determined the increase of local symmetry of  $\text{BO}_6$  groups and the increase of polarity of Mn-O bonds which can be determined by the increase of  $\text{Mn}^{3+}$  concentration and/or the supplementary polarization (dipole moment) due to local distortion of the the lattice near the grain boundary.

The range of broad frequencies ( $\Delta\nu_{\text{Mn-O}}$ ) increase with the increases of Fe/Mn ratio concentration. This process is due to the light decrease of average grain size.

Diffuse reflectance spectra (DRS) were measured to know variation of the band gap in compounds and the d-d transition energy of  $\text{Mn}^{3+}$ ,  $\text{Mn}^{4+}$ ,  $\text{Fe}^{2+}$  and  $\text{Fe}^{3+}$ . The magnitude of band gap depends on ionicity of bonding in solid. The DRS of LHSMFO and LHCMFO samples are shown in Fig. 2.

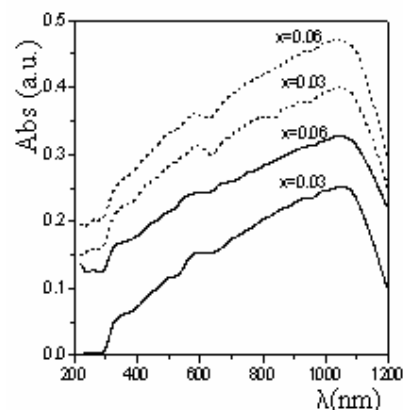


Fig. 2. Diffuse reflectance spectra of LHSMFO (solid lines) and LHCMFO (dashed lines) manganites.

Absorption edges, which are designated as the wavelength having maximum derivatives of reflectance, are positioned at 1054 nm ( $x=0.03$ ) and 1046 nm ( $x=0.06$ ) for LHSMFO, 1042 nm ( $x=0.03$ ) and 1036 nm ( $x=0.06$ ) for LHCMFO. The small oxidizing power of  $\text{Fe}^{3+}$  ( $d^5$ ,  $^5S$  ground term) relative to  $\text{Mn}^{4+}$ , charge transfer (CT) bands of Fe cations often obscure the very low intensity of d-d  $\text{Fe}^{3+}$  absorption (for non-symmetric  $\text{FeO}_6$  octahedra). The iron ions are in paramagnetic high-spin configuration at room temperature.

The spectra of LHSMFO with  $x=0.03$  shows a spectra of manganites with a high concentration of  $\text{Mn}^{3+}$  ions.

The increase of Fe content in the samples determined a significant decreasing of intensity of absorption of d-d and charge transfer bands in 600-1100 nm range. There are counterbalanced by the increase of CT  $\text{Fe}^{3+}\text{-O}^{2-}$  from 300 – 600 nm range. It is assumed that the absorption edges observed in 600-1100 nm range are due to absorption of  $\text{Fe}^{3+}$  and  $\text{Mn}^{3+/4+}$  d-d transition ( $\text{Mn}^{3+}$ :  $^5E_g \rightarrow ^5T_{2g}$ ;  $\text{Mn}^{4+}$ :  $^4A_{2g} \rightarrow ^4T_{2g}$ ,  $^4A_{2g} \rightarrow ^4T_{1g}$ ) and charge transfer of  $\text{Mn}^{3+}$  and  $\text{Mn}^{4+}$  to  $\text{O}^{2-}$  in which an electron is transferred from the

highest filled molecular orbital (localized on the oxide ions) to the lowest empty molecular orbital (localized on the manganese ion). The higher Fe atoms content determined decreasing of  $Mn^{3+}$  concentration. In perovskites structure, the oxide ions are coordinated by B and A ions. Hence, by considering the fact that the 2p orbital can be directed toward A site ions, it is reasonable for the CT absorption bands of A-O to depend on B site ion. The CT absorption bands of Ln-O and (Sr, Ca)-O shifted to smallest wavelength. The increase of contribution of the Ln-O bonds is induced to the increases of  $Fe^{3+}$  concentration from the sample, which is able to give more electron cloud to oxide ion, the Mn-O bond becomes more covalent and increasing of  $Mn^{4+}$  can be facilitated. This is a reasonable explanation of the diminish of the intensities of the transition d-d and CT of  $Mn^{3+}$ .

Magnetic measurement, performed between 77 and 300 K indicate a decrease of the molar magnetization vs increase Fe concentration or when Ca substitutes Sr in the samples (s. Fig.3).

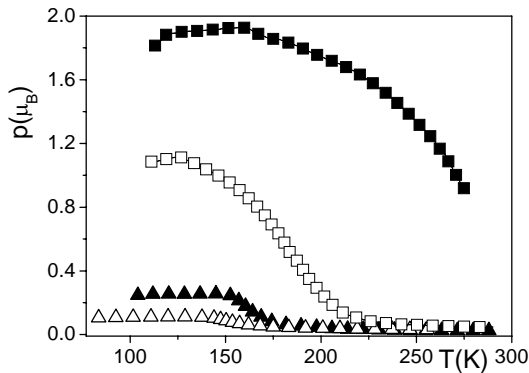


Fig. 3. The variation of molar magnetization vs temperature and Fe concentration for LHSMFO/LHCMFO (Sr doped manganites: ■ -  $x=0.03$  and □ -  $x=0.06$ ; Ca doped manganites: ▲ -  $x=0.03$  and △ -  $x=0.06$ ).

We consider that the cation distribution is given by the relation:



The dependence of maximum specific magnetization is given by the relation:

$$p_{max} = 3.65 - 4x - 2\delta \quad (2)$$

if to the magnetic moment of the sample participate all Mn cations, or:

$$p_{max} = 2.45 - 14\delta \quad (3)$$

if to the magnetic moment participate only  $Mn^{3+}$ - $Mn^{4+}$  pairs. Only Eq. (3) can satisfy the observed values of the molar magnetization, Eq.(2) can given the observed molar magnetization only for very large values of the oxygen

deficit in the samples (such deficits were not observed). A more complex scenario is possible if we consider that a part of  $Mn^{4+}/Mn^{3+}$  take part to the  $Mn^{4+}$ -O- $Fe^{4+}$  or  $Mn^{3+}$ -O- $Fe^{3+}$  superexchange interactions, that means the appearance of antiferromagnetic regions. Because  $Mn^{3+}/Fe^{3+}$  or  $Mn^{4+}/Fe^{4+}$  have different magnetic moments, a net magnetic moment can results for the antiferromagnetic zone. We intend to perform neutron diffraction on these samples, to clarify the electronic phase composition of our samples. However, the observed variation of the molar magnetization can be better explained by considering only the  $Mn^{3+}$ - $Mn^{4+}$  pairs contribution to the magnetic moment (s. Eq.(3)). In agreement with the literature data we have not take in account the magnetic moment of  $Mn^{3+}$ - $Fe^{3+}$  or similar pairs. On other hand the decrease of the Curie temperature with increase of Fe concentration in the Sr doped manganites can be attributed to a decrease of the double exchange interaction as comparing with superexchange interaction (s.Tab.1). Because the substitution of  $Mn^{3+}$  with  $Fe^{3+}$  does not modify the B-O distances, only one reason exists to induce a behavior: the presence of  $Fe^{3+}$  promote a superexchange interaction.

Table 1. Dependence of the lattice constants Curie temperature ( $T_C$ ) and maximum molar magnetization ( $P_{max}$ ) with the Fe concentration ( $x$ ) in LHSMFO/LHCMFO manganites.

x	Sr		Ca	
	$T_C$ (K)	$P_{max}$ ( $\mu_B$ )	$T_C$ (K)	$P_{max}$ ( $\mu_B$ )
0.03	>300	1.90	161	0.26
0.06	180	1.11	149	0.11

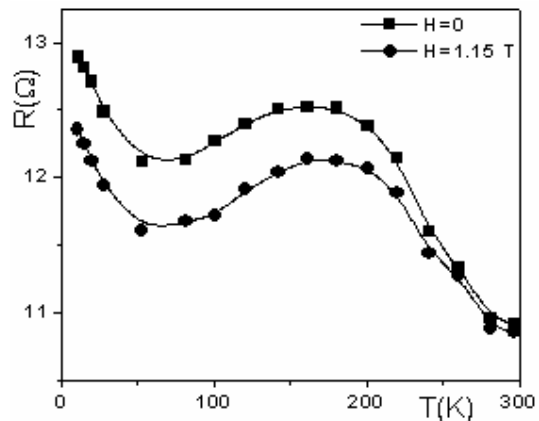


Fig. 4. Variation of the resistance vs T and applied magnetic field for doped with Sr samples ( $x_e=0.03$ ).

A spin-glass behaviour appeared for the samples doped with Sr (s. Fig. 3).

Substitution of Sr ( $r_{Sr^{2+}}=1.45 \text{ \AA}$ ) with Ca ( $r_{Ca^{2+}}=1.32 \text{ \AA}$ ) decreases the tolerance factor and increase the disorder in

the second coordination sphere of Mn cations, implicitly to a decrease of the Mn-O-Mn DE interactions and a decrease of Curie temperature (s. Fig. 3) for the samples with the same Fe concentration.

Relative increase of superexchange (SE) interactions leads to an increase of antiferromagnetic ordered magnetic moments and a decrease of molar magnetization.

These suppositions are confirmed by the transport measurements on the Sr/Ca substituted samples (s. Fig. 4, 5 and 6). The Sr doped samples present a net transition from the metallic to insulator state, while the Ca doped samples behave as insulators.

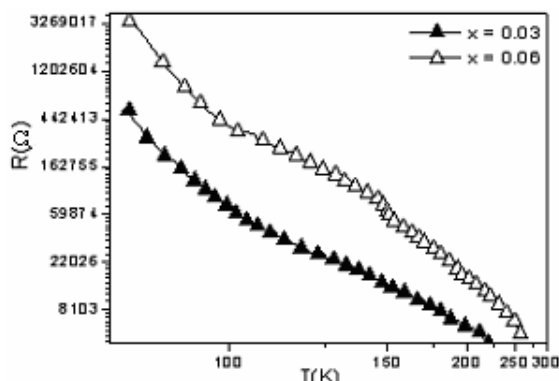


Fig. 6. Variation of the resistance vs  $T$  and applied magnetic field for doped with Ca samples ( $x=0.06$ ).

Transition temperature from metal to insulator ( $T_{MI}$ ) have a small decrease with the increase of Fe concentration in the Sr doped samples ( $C_{Fe}$ ), while the magnetoresistance increases two times (s. Fig. 2 and 3). At low temperature ( $T < 50$  K) in the Sr doped manganites it appears a large magnetoresistance, which was attributed to the spin-glass state (s. Fig. 1, 2 and 3). If a small substitution of Mn with Fe have a little influence on the resistance of the sample, in the absence of the magnetic field, the substitution of Sr with Ca determine an increase of resistance by  $10^5$  (s. Fig. 4). The applied magnetic field shows no influence on the values of resistance. A large maximum of resistance, superposed on variation of semiconductor type, was observed for both Ca doped manganites. The temperature associated to this maximum moves to higher values with the increase of the Fe concentration.

#### 4. Conclusions

We have prepared a raw of  $La_{0.54}Ho_{0.11}(Sr/Ca)_{0.35}Mn_{1-x}Fe_xO_3$  manganites by sol-gel methods. Fe influences indirectly the appearance and increasing, when the Fe concentration increases, of antiferromagnetic region and to the decrease of the DE interactions as comparing with SE interactions. This process takes place, despite the very small difference between the crystallographic radii of these two cations.

The substitution of Mn with Fe leads to an increase disorder on B places, associated with an increase of magnetoresistance, for Sr doped manganites. From UV-VIS and IR measurements we can conclude that the increase of the Fe/Mn ratio determined a symmetry increase of the  $BO_6$  octahedra, respectively, of the crystalline lattice. This is associated with an increase of the (Mn, Fe)-O bond polarity and a decrease of the  $Mn^{3+}$  concentration.

We suppose that the  $La_{0.54}Ho_{0.11}(Sr/Ca)_{0.35}Mn_{1-x}Fe_xO_3$  manganites are formed from a antiferromagnetic insulator matrix, with ferromagnetic-metallic droplets, the ferromagnetic domains being larger in the Sr doped manganites. The change of Sr with Ca leads to large distortions in the second coordination sphere of B cations and, implicitly to a decrease of the DE interactions as comparing with the SE interactions.

#### References

- [1] C. Zener, Phys. Rev. **82**, 403 (1951).
- [2] Y. L. Chang, C. K. Ong, Appl. Phys. Lett. **81**, 1721 (2003).
- [3] M. Pissas, G. Kallias, Phys. Rev. **B 68**, 134414 (2003).
- [4] P. M. Woodward, T. Vogt, D. E. Cox, A. Arulraj, C. N. R. Rao, P. Karen, A. K. Cheetham, Chem. Mater. **10**, 3652 (1998).
- [5] X. H. Li, Y. H. Huang, C. H. Yan, Z. M. Wang, C. S. Liao, J. Phys.: Condens. Matter **14**, L177 (2002).
- [6] F. Chen, H. W. Liu, K. F. Wang, H. Yu, S. Dong, X. Y. Chen, X. P. Jiang, Z. F. Ren, J-M Liu, J. Phys.: Condens. Matter **17**, L467 (2005).
- [7] K. H. Ahn, X. W. Wu, K. Liu, C. L. Chien, Phys. Rev. **B 54**, 299 (1996).
- [8] A. Simopoulos, M. Pissas, G. Kallias, E. Devlim, N. Moutis, I. Panagiotopoulos, D. Niarchos, C. Christides, R. Sonntag, Phys. Rev. **B 59**, 1263 (1999).
- [9] S. B. Ogale, R. Shreekala, Ravi Bathe, S. K. Date, S. I. Patil, B. Hannoyer, F. Petit, G. Marest, Phys. Rev. **B 57**, 7841 (1998).
- [10] M. L. Craus, M. Lozovan, C. Baci, J. Optoelectron. Adv. Mater. **9**(5), 1582 (2007).
- [11] M. L. Craus, N. Cornei, J. Optoelectron. Adv. Mater. **9**(6), 1736 (2007).

\* Corresponding author: loz@phys-iasi.ro